

# Spectral properties and supramolecular inclusion complexes of $\beta$ -cyclodextrin with flexible amphiphilic and rigid compounds

Xinzhen Du\*, Weihua Lu, Ning Ding, Hongxia Dai, Xiulan Teng, Hualin Deng

*Department of Chemistry, Northwest Normal University, Lanzhou 730070, PR China*

Received 2 January 2005; received in revised form 4 April 2005; accepted 6 May 2005

Available online 15 June 2005

## Abstract

Spectral properties and inclusion complexes of  $\beta$ -cyclodextrin ( $\beta$ -CD) with nonionic amphiphiles and rigid 1-bromonaphthalene (BrN) was investigated in detail. Fluorescence and  $^1\text{H}$  NMR measurements give new insights into inclusion of the hydrophobic moiety of amphiphiles into the cavity of  $\beta$ -CD. Their apparent stability constants were well correlated with the structure of the hydrophobic moiety of amphiphiles. The long and flexible hydrophobic moiety may occupy the cavity in the compressed manner. The phosphorescence quenching and the binding strength of BrN in ternary complexes indicate that the inclusion depth and the rigidity of BrN in the cavity of  $\beta$ -CD are predominant factors in determining its phosphorescence. Further inclusion of rigid BrN into the cavity drives the built-in phenyl group of amphiphiles to expose to bulk water phase to a greater extent. Comparative analyses of molecular sizes and models reveal that the flexible hydrocarbon chain of an amphiphile in supramolecular inclusion complexes was located inside the crowded cavity of  $\beta$ -CD due to the filling of rigid BrN into the cavity.

© 2005 Elsevier B.V. All rights reserved.

**Keywords:**  $\beta$ -Cyclodextrin; Amphiphiles; Supramolecular inclusion complexes; Fluorescence; Phosphorescence;  $^1\text{H}$  NMR

## 1. Introduction

Cyclodextrins (CDs) are macrocyclic  $\alpha$ -1,4-maltooligosaccharides consisting of D-(+)-glucopyranose units. With their special molecular structures, they are capable of incorporating various organic compounds into their nanocavities and affecting the physical and chemical properties of incorporated compounds. Thus, CDs have been used in many fields such as foods, cosmetics, toiletries, agrochemicals and pharmaceuticals based on inclusion of CDs with functional compounds [1,2]. Since amphiphiles are usually employed in above areas, amphiphiles may have a significant effect on the inclusion of functional compounds for the preferential binding of amphiphiles over functional compounds to the cavity of CDs. Among CDs,  $\beta$ -cyclodextrin ( $\beta$ -CD) composed of seven glucopyranose units is most popular. Many researchers have studied the interaction of  $\beta$ -CD with amphiphiles and the corresponding thermodynamic parameters by conduc-

tance [3–12], surface tension [11–16], spectroscopy [17–28] and other methods [29–33]. However, few reports dealt with structural analysis of supramolecular inclusion complexes of CDs with amphiphiles in detail [12,34,35]. Especially, the influence of flexible amphiphiles on the inclusion of the second rigid molecule into the CD cavity is helpful to better understand the development and applications of CDs in above described fields. For these reasons, different structural amphiphiles with and without aromatic chromophore and bromonaphthalene were artfully selected to comparatively study the supramolecular inclusion of  $\beta$ -CD with flexible and rigid compounds. Different fluorescence and  $^1\text{H}$  NMR of amphiphiles included by  $\beta$ -CD allows to evaluate the binding sites of an amphiphile to  $\beta$ -CD cavity. Bright phosphorescence of 1-bromonaphthalene (BrN) included in the cavity of  $\beta$ -CD provides further information about the interaction between a linear amphiphile and a pie-like BrN and the binding site of BrN to  $\beta$ -CD cavity in supramolecular inclusion complexes since the phosphorescence is extremely sensitive to the microenvironment around its excited triplet state. Comparison of molecular sizes is also helpful to

\* Corresponding author. Tel.: +86 931 7972194; fax: +86 931 7972194.  
E-mail address: [xinzhendu@yahoo.com](mailto:xinzhendu@yahoo.com) (X. Du).

understand the reasonable supramolecular inclusion models in aqueous solution.

## 2. Experimental

$\beta$ -Cyclodextrin, polyethylene glycol ( $n=10$ ) *tert*-octylphenyl ether (commercially Triton X-100, TX) and its reduced form (TX(R)) were obtained from Sigma and used as received. Polyethylene glycol ( $n=10$ ) *n*-octylphenyl ether (commercially OP) was obtained from Shanghai Reagent Company. *n*-Octanol (Oct) and phenolphthalein (PP) of analytical grade were purchased from Tianjin Reagent Company and PP was recrystallized twice in ethanol prior to use. 1-Bromonaphthalene was obtained from Beijing Zhonglian Fine Chemicals and distilled under reduced pressure. BrN of  $2.5 \times 10^{-5}$  M was employed throughout the experiments. Potassium iodide was newly prepared prior to use. Doubly distilled water was used in the experiment.

All steady state fluorescence and phosphorescence spectra were performed on Shimadzu RF-540 recording fluorescence spectrophotometer equipped with a 150 W xenon lamp as an excitation light source and a thermostated cell holder. Excitation and emission bandpasses of 5 nm were employed. Absorption spectra were obtained with Hitachi U-3400 spectrophotometer.  $^1\text{H}$  NMR studies were carried out in  $\text{D}_2\text{O}$  on a Varian Inova-400 MHz spectrometer. For estimation of apparent stability constants and quenching measurements, the temperature was kept at  $25^\circ\text{C}$ . Molecular dimensions and models were estimated by Chem3D software of CambridgeSoft.

## 3. Results and discussion

### 3.1. Fluorescence of amphiphiles and their inclusion complexes

Of four amphiphiles, OP and TX show fluorescence due to their built-in aromatic chromophore and was used as the probes to monitor the inclusion of  $\beta$ -CD with amphiphiles. As shown in Fig. 1a, OP only shows 305 nm fluorescence with the excitation maximum of 277.6 nm below  $5.0 \times 10^{-5}$  M. However, OP shows another broad featureless 355 nm fluorescence with the excitation maximum of 284 nm around  $1.0 \times 10^{-4}$  M, which is very close to its critical micelle concentration (CMC) [36]. Since OP molecules were homogeneously distributed in aqueous solution at  $2.5 \times 10^{-5}$  M, the fluorescence at 305 nm can be ascribed to OP monomers. The 355 nm fluorescence should be assigned to OP aggregates. In the presence of  $\beta$ -CD, the 355 nm fluorescence of OP was gradually attenuated whereas the monomer-like fluorescence of OP at about 302 nm was greatly enhanced. For  $5.0 \times 10^{-4}$  M OP, the fluorescence of aggregates almost disappears in the presence of  $5.0 \times 10^{-4}$  M  $\beta$ -CD (Fig. 1b). These experimental phenomena suggest that the channeled cavity of  $\beta$ -CD include the *n*-octyl chain of OP responsible

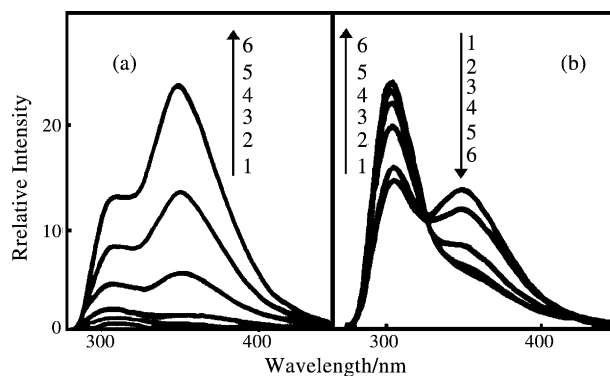


Fig. 1. Fluorescence spectra of OP in the (a) absence and (b) presence of  $\beta$ -CD: (a) (1)  $2.5 \times 10^{-5}$  M; (2)  $5.0 \times 10^{-5}$  M; (3)  $1.0 \times 10^{-4}$  M; (4)  $2.5 \times 10^{-4}$  M; (5)  $5.0 \times 10^{-4}$  M; (6)  $1.0 \times 10^{-3}$  M OP and (b)  $5.0 \times 10^{-4}$  M OP; (1)  $5.0 \times 10^{-5}$  M; (2)  $1.0 \times 10^{-4}$  M; (3)  $2.5 \times 10^{-4}$  M; (4)  $5.0 \times 10^{-4}$  M; (5)  $7.5 \times 10^{-4}$  M; (6)  $1.0 \times 10^{-3}$  M  $\beta$ -CD.

for the aggregation of OP. In this case, OP included by  $\beta$ -CD loses its unique amphiphilicity. The spectral changes provide additional evidence for the conclusion that the hydrophobic moieties of amphiphiles are buried into the cavity obtained by conductance and surface tension [11].

In addition, the enhanced monomer-like fluorescence of OP and TX below CMC also shows the slight bathochromic shift of excitation maximum and the slight hypochromic shift of emission maximum in the presence of excess  $\beta$ -CD compared to free OP and TX. This spectral behavior resembles that of phenolic derivatives in water and dioxane, respectively [37]. It reveals that the phenyl ring between the octyl chain and polyethylene glycol was located in less polar CD cavity compared to water phase. In homogeneous solutions, the dynamic fluorescence quenching was examined by the following Stern–Volmer equation:

$$\frac{I_0}{I} = 1 + K_{SV}[Q]$$

where  $I_0$  and  $I$  are the fluorescence intensities in the absence and presence of quencher, respectively,  $K_{SV}$  the quenching

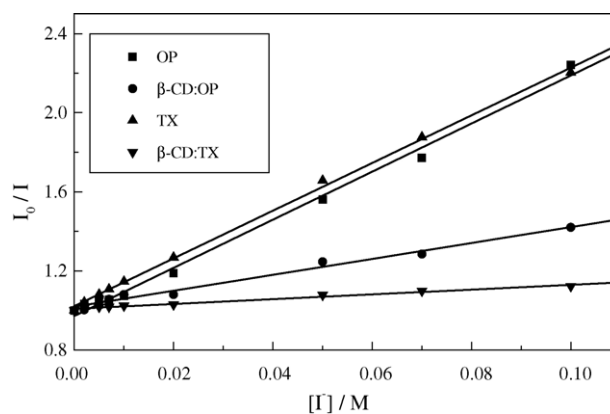


Fig. 2. Stern–Volmer plots of  $I_0/I$  vs.  $[I^-]$  for  $\beta$ -CD:OP and  $\beta$ -CD:TX complexes— $5.0 \times 10^{-5}$  M OP and TX and  $1.0 \times 10^{-3}$  M  $\beta$ -CD.

constant and  $[Q]$  is quencher concentration. As shown in Fig. 2, the fluorescence from the phenyl groups of OP and TX was greatly shielded from iodide ions in the presence of excess  $\beta$ -CD compared to free OP and TX. Especially, TX only shows very small fluorescence quenching by iodide ions. This provides direct evidence that the phenyl groups of OP and TX were entrapped into the cavity of  $\beta$ -CD together with their octyl chains. However, the phenyl group of OP and TX is close to the cavity opening because the fluorescence quenching is suppressed to some extent.

### 3.2. $^1\text{H}$ NMR spectra of amphiphiles and their inclusion complexes

$^1\text{H}$  NMR shifts are particularly suited to follow several signals for characterization of supramolecular inclusion of amphiphiles in the cavity of  $\beta$ -CD. Fig. 3 shows  $^1\text{H}$  NMR spectra of  $\beta$ -CD, TX and  $\beta$ -CD:TX complex in  $\text{D}_2\text{O}$ . Addition of  $\beta$ -CD to TX solution results in significant  $^1\text{H}$  downfield shift differences up to 0.193 for  $\alpha$ -CH<sub>3</sub>, 0.118 for  $\beta$ -CH<sub>2</sub>, 0.092 for  $\gamma$ -CH<sub>3</sub> of *tert*-octyl chain as well as

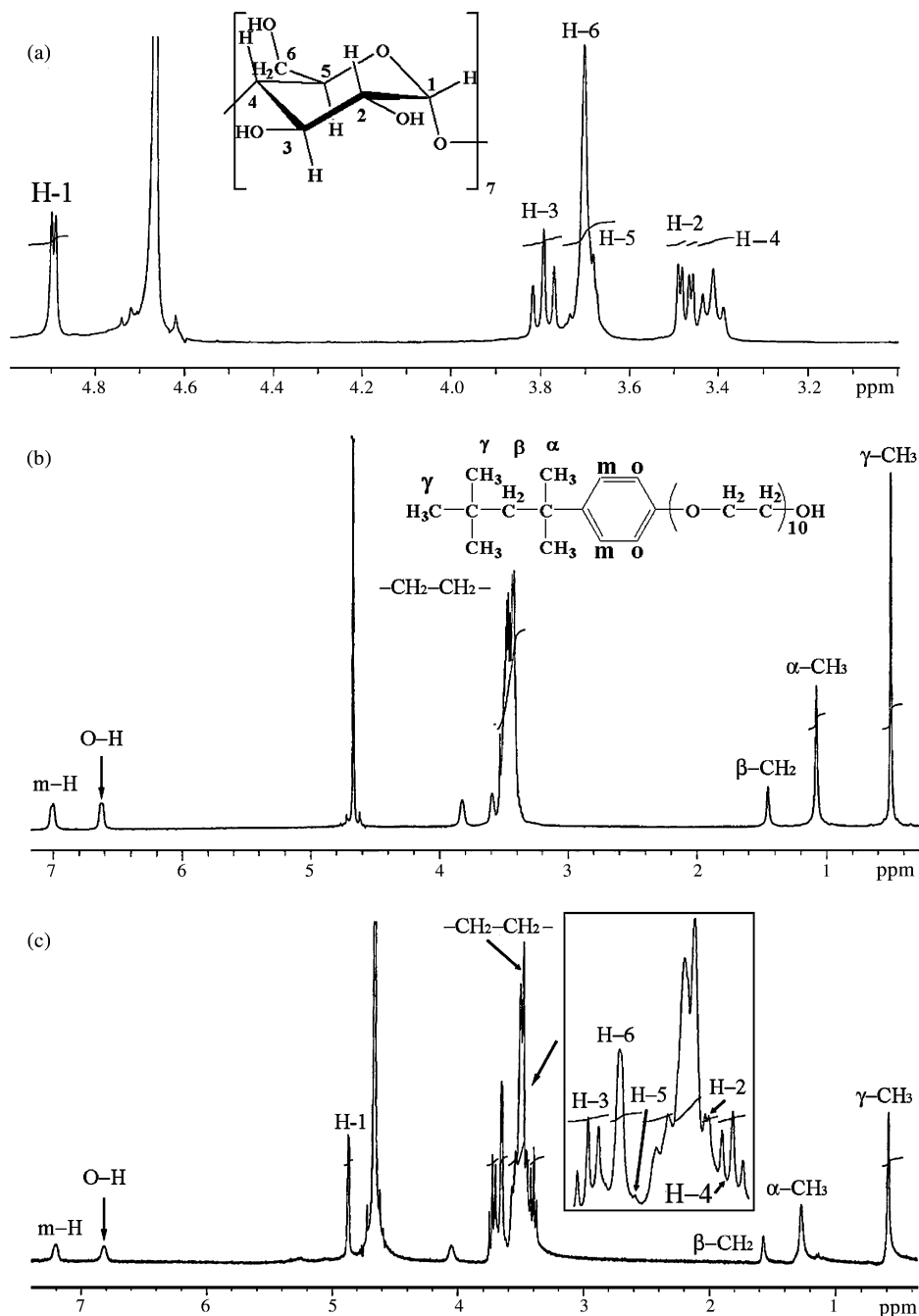


Fig. 3.  $^1\text{H}$  NMR of: (a)  $\beta$ -CD; (b) TX; (c)  $\beta$ -CD:TX complex.

0.207 for *o*-H and 0.204 for *m*-H of phenyl ring compare to those of individual TX, respectively.  $\beta$ -CD also shows remarkable  $^1\text{H}$  upfield shifts from  $\delta 3.794$  to  $\delta 3.729$  for H-3 signals (triplet) and from  $\delta 3.683$  to  $\delta 3.660$  for H-5 signals (singlet) at the same time. However, TX has negligible effect on H-1, H-2, H-4 and H-6 directed outside the cavity. Such proton shifts are generally believed to indicate the inclusion of hydrophobic moiety in the cavity of  $\beta$ -CD [38,39]. The experimental data provide additional evidence for inclusion of *tert*-octyl chain and phenyl group of TX in the cavity of  $\beta$ -CD. The same results were obtained for  $\beta$ -CD:TX(R) complex. In the case of  $\beta$ -CD:OP and  $\beta$ -CD:Oct complexes, corresponding proton shift differences are relatively smaller.

### 3.3. Phosphorescence of $\beta$ -CD complexes with amphiphiles and BrN

Under the experimental conditions, BrN shows no phosphorescence in aqueous solution of an amphiphile or  $\beta$ -CD. Bright phosphorescence of BrN can be observed in the presence of Oct, OP, TX or TX(R) and  $\beta$ -CD, indicating that the supramolecular inclusion complexes were formed in aqueous solutions. The phosphorescence intensity of BrN increases in ternary inclusion complexes including OP, Oct, TX and TX(R). Furthermore, amphiphile-assisted inclusion of  $\beta$ -CD with BrN also results in a great bathochromic shift of excitation maximum from 279 nm of free BrN to 299 nm of included one. In particular, the phosphorescence of BrN was also observed for the  $\beta$ -CD:TX:BrN complex when TX was irradiated at 264 nm. Fig. 4 shows the fluorescence quenching of TX (Fig. 4a) along with the phosphorescence enhancement of BrN (Fig. 4b) with increasing concentration of BrN. Clearly, the energy transfer between the phenyl group of TX and BrN occurs. For the  $\beta$ -CD:OP:BrN complex, BrN has similar quenching effect on fluorescence of OP but shows no phosphorescence when OP was irradiated. These results indicate that the phenyl groups of OP and TX were located in the proximity of BrN in the complexes because the energy transfer and the fluorescence quenching is an intermolecular process dependent on the distance between the phenyl group and BrN. Phosphorescence quenching measurements give new insight into the microenvironmental nature of excited BrN in supramolecular inclusion complexes (Table 1). In the presence of *n*-octanol, the best protection of BrN from iodide ions was obtained. Iodide ions show the most significant quenching effect on the phosphorescence of BrN in the presence of TX(R). This suggests that BrN

Table 1  
Stern–Volmer phosphorescence quenching constants for supramolecular inclusion complexes

Complexes	$K_{SV}$ ( $\text{M}^{-1}$ )
$\beta$ -CD:Oct:BrN	$0.26 \pm 0.28$
$\beta$ -CD:OP:BrN	$10.06 \pm 0.37$
$\beta$ -CD:TX:BrN	$68.33 \pm 2.15$
$\beta$ -CD:TX(R):BrN	$1564.78 \pm 51.05$

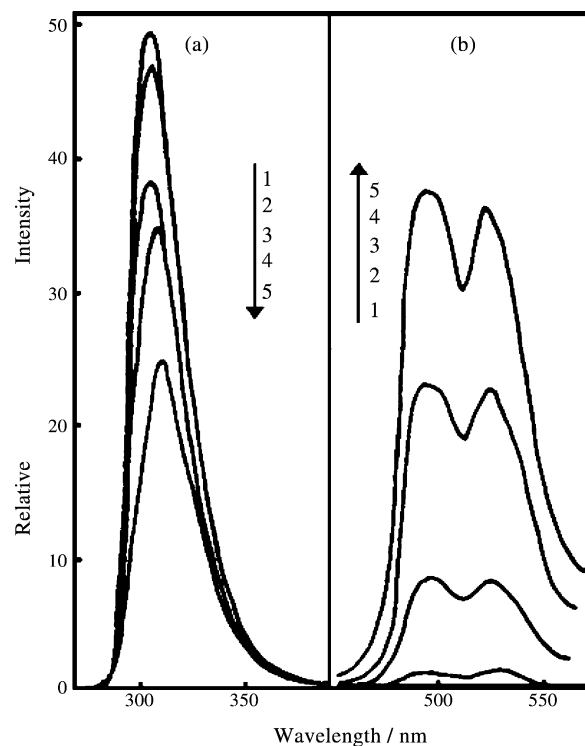
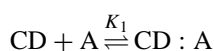
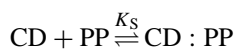


Fig. 4. Fluorescence of: (a) TX and phosphorescence of (b) BrN from  $\beta$ -CD:TX:BrN complex:  $3.0 \times 10^{-3}$  M  $\beta$ -CD,  $2.5 \times 10^{-3}$  M TX and BrN—(1) 0; (2)  $5.0 \times 10^{-6}$  M; (3)  $2.5 \times 10^{-5}$  M; (4)  $6.25 \times 10^{-5}$  M; (5)  $1.25 \times 10^{-4}$  M; excitation, 264 nm.

should be exposed to bulk water phase to the greatest extent in  $\beta$ -CD:TX(R):BrN complex.

### 3.4. Inclusion of $\beta$ -CD with amphiphiles and BrN

*n*-Octanol and TX(R) do not have any chromophore in the ultraviolet and visible regions of the spectrum. For this purpose, a spectral method based on the displacement of PP from the cavity of  $\beta$ -CD was employed to determine stability constants of  $\beta$ -CD with amphiphiles [30,40]. Free PP dianion in quinone phenolate in solution is purple at pH  $\sim 10.5$  and shows absorption maximum at 548 nm. However, the 1:1 complex of  $\beta$ -CD with PP has an absorbance practically equal to zero around 548 nm because the formation of lactone ring is induced on inclusion [41]. Apparent stability constants ( $K_S$ ) for the complex of  $\beta$ -CD with PP was calculated to be  $(2.71 \pm 0.08) \times 10^4 \text{ M}^{-1}$  by fitting spectroscopic data, which is very close to the literature value [30,40]. PP is displaced from the cavity of  $\beta$ -CD when an amphiphile (A) was added to aqueous solution containing  $\beta$ -CD and PP. Fig. 5 shows the dependence of typical absorbance of PP on  $\beta$ -CD and OP. In aqueous solution, the related competitive equilibrium can be expressed by the following equations:



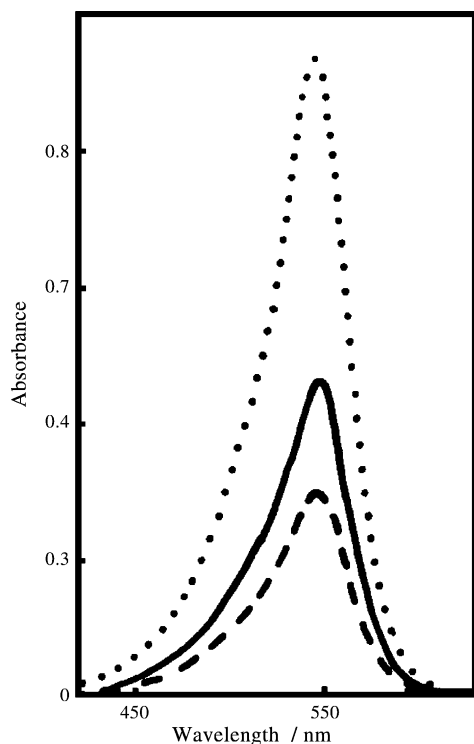


Fig. 5. Absorption spectra of PP in the presence of  $\beta$ -CD and OP. PP ( $\cdots$ ), PP +  $\beta$ -CD ( $---$ ) and PP +  $\beta$ -CD + OP ( $—$ ):  $3.0 \times 10^{-5}$  M PP,  $1.0 \times 10^{-4}$  M  $\beta$ -CD and  $2.0 \times 10^{-4}$  M OP.

By measuring the increase in absorbance at 548 nm in the presence of an amphiphile, apparent stability constants ( $K_1$ ) were evaluated by nonlinear least-square fitting method. As shown in Table 2, the values of  $K_1$  increase in the order Oct < OP < TX < TX(R). The inclusion of phenyl ring of OP contributes to the thermodynamic stability to a certain extent compared to *n*-octanol. Furthermore, the *tert*-octyl chain of TX has a greater affinity for the interior of  $\beta$ -CD than the *n*-octyl chain of OP. The cyclohexyl ring of TX(R) has a stronger interaction with the cavity of  $\beta$ -CD. These data demonstrate that the binding strength greatly depends on the nature of the hydrophobic moiety of amphiphiles.

For amphiphile-assisted inclusion of  $\beta$ -CD with BrN, the inclusion equilibrium was represented by the following equation:

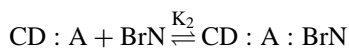


Table 2  
Apparent stability constants of  $\beta$ -CD:A complexes

Complexes	$K_1$ ( $\text{M}^{-1}$ )
$\beta$ -CD:Oct	$(1.49 \pm 0.39) \times 10^3$
$\beta$ -CD:OP	$(7.37 \pm 1.83) \times 10^3$
$\beta$ -CD:TX	$(1.82 \pm 0.15) \times 10^5$
$\beta$ -CD:TX(R)	$(3.90 \pm 0.36) \times 10^5$

Table 3  
Apparent stability constants of  $\beta$ -CD:A:BrN complexes

Complexes	$K_2$ ( $\text{M}^{-1}$ )
$\beta$ -CD:Oct:BrN	$(5.05 \pm 0.75) \times 10^2$
$\beta$ -CD:OP:BrN	$(1.23 \pm 0.29) \times 10^2$
$\beta$ -CD:TX:BrN	$(1.49 \pm 0.18) \times 10^2$
$\beta$ -CD:TX(R):BrN	$(2.71 \pm 0.43) \times 10^3$

The following modified Benesi–Hildebrand expression was derived according to literature [42]:

$$\frac{1}{\Delta I_P} = \frac{1}{aK_2[A]} + \frac{1}{a}$$

where  $\Delta I_P$  is the difference in phosphorescence intensity of BrN in the presence and absence of an amphiphile at fixed concentration of  $\beta$ -CD,  $a$  the combined instrumental constant and  $[A]$  is the equilibrium concentration of an amphiphile. The double reciprocal plots of  $1/\Delta I_P$  versus  $1/[A]$  were linear for all supramolecular inclusion complexes. The ratio of intercept to slope affords to evaluate their values of  $K_2$  in Table 3. As compared with that  $((7.02 \pm 0.29) \times 10^2 \text{ M}^{-1})$  of  $\beta$ -CD:BrN complex, the smaller values of  $K_2$  were obtained for  $\beta$ -CD:Oct:BrN,  $\beta$ -CD:OP:BrN and  $\beta$ -CD:TX:BrN complexes, suggesting that the binding strength of BrN decrease. Interestingly the value of  $K_2$  increases in the case of TX(R).

### 3.5. Supramolecular inclusion complexes of $\beta$ -CD with flexible amphiphiles and rigid BrN

Molecular sizes and models are helpful to fully understand supramolecular inclusion of  $\beta$ -CD with flexible amphiphiles and rigid BrN. Fig. 6 presents the cylindrical bonding models of  $\beta$ -CD, *n*-octanol, OP, TX and TX(R). In the case of *n*-octanol and OP, the cross-section of the cylindrical *n*-octyl chain corresponds to the diameter of 4.50 Å. Clearly, it is smaller than the diameter ( $D$ , Å) of  $\beta$ -CD cavity ( $D = 6.5$  Å) [1]. The channeled cavity of  $\beta$ -CD is wide enough to include the *n*-octyl chain. In terms of the length ( $L$ , Å) of *n*-octyl chain and the depth (7.9 Å) of  $\beta$ -CD cavity, however, the long and fine *n*-octyl chain ( $L = 10.55$  Å) is not completely included into the cavity and the phenyl ring of OP should stay in bulk solution. This geometric arrangement cannot account for the fluorescence enhancement and  $^1\text{H}$ NMR shifts of OP in the presence of  $\beta$ -CD. The long and flexible *n*-octyl chain may occupy the cavity in the compressed manner so as to further include appended phenyl ring into the cavity. Thereby, the fluorescence quenching of OP by iodide ions was greatly reduced and the value of  $K_1$  of  $\beta$ -CD:OP complex was increased in comparison with that of the  $\beta$ -CD:Oct complex. In the case of TX and TX(R), the cylindrical size of the *tert*-octyl chain approximately equals 5.79 Å. The short and bulky *tert*-octyl chain ( $L = 5.50$  Å) with the phenyl ring ( $L = 2.82$  Å) of TX or the cyclohexyl ring ( $L = 2.92$  Å) of TX(R) is better fit to the channeled cavity and may be encapsulated into the cavity of  $\beta$ -CD. Lower fluorescence quenching of the phenyl



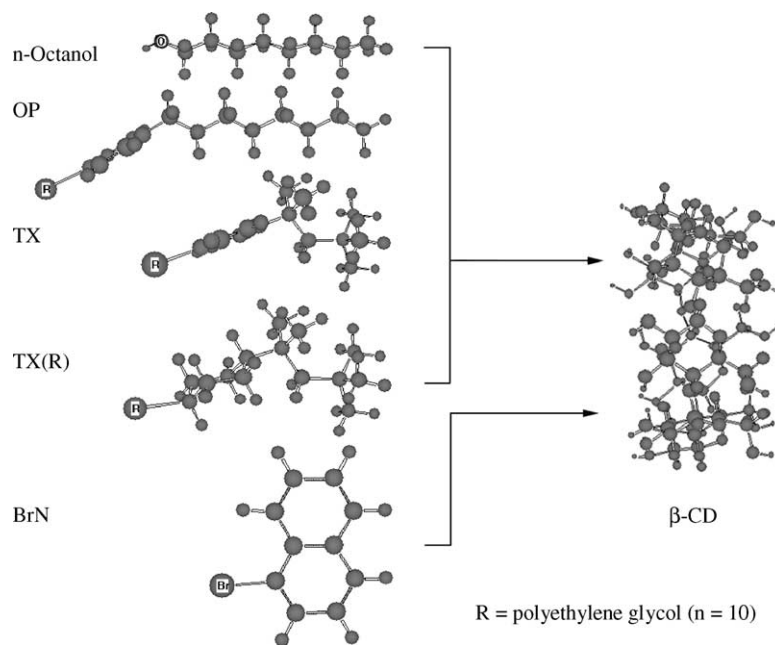


Fig. 6. Cylindrical bonding models of  $\beta$ -CD, *n*-octanol, OP, TX and TX(R).

ring of TX by iodide ions, greater  $^1\text{H}$  NMR shift differences and much larger value of  $K_1$  support this spatial arrangement. Especially, the cyclohexyl ring of TX(R) was more easily included into the cavity than the phenyl ring of TX due to its lower polarity and the  $\beta$ -CD:TX(R) complex shows the greatest thermodynamic stability.

According to overall molecular sizes ( $V$ ,  $\text{\AA}^3$  for volume) of the *n*-octyl chain of *n*-octanol ( $V = 167.71 \text{\AA}^3$ ), the *n*-octyl chain with phenyl group of OP ( $V = 224.69 \text{\AA}^3$ ), the *tert*-octyl chain with phenyl group of TX ( $V = 201.72 \text{\AA}^3$ ), the *tert*-octyl chain with cyclohexyl group of TX(R) ( $V = 233.45 \text{\AA}^3$ ) and BrN ( $V = 171.55 \text{\AA}^3$ ), the void space in the cavity of  $\beta$ -CD ( $V = 262 \text{\AA}^3$ ) fails to further incorporate BrN into the cavity occupied by the hydrophobic moiety of an amphiphile. Further inclusion of rigid BrN into the cavity could drive the phenyl ring of OP and TX to expose to bulk water phase to a greater extent. The polar microenvironment will result in the bathochromic shift of emission maximum ( $\lambda_{\text{em}}$ ) of the phenyl rings of OP and TX according to the effect of solvent on the fluorescence of phenolic derivatives [37]. The experimental data in Table 4 prove to be true for this inference based on geometric considerations. For this reason, BrN

Table 4  
Bathochromic shift of  $\lambda_{\text{em}}$  of OP and TX in supramolecular inclusion complexes

Concentration of BrN/M	$\lambda_{\text{em}}$ (nm)	
	$\beta$ -CD:OP:BrN	$\beta$ -CD:TX:BrN
No	302.4	303
$5.0 \times 10^{-6}$	302.8	303.5
$1.0 \times 10^{-5}$	303.2	303.8
$2.5 \times 10^{-5}$	304.3	304.8
$5.0 \times 10^{-5}$	306.2	306

also fails to be deeply included into the constrained cavity of  $\beta$ -CD due to the spatial effect. Furthermore, the larger size and the preferential binding of hydrophobic moiety to the cavity could also drive BrN to expose to bulky water phase to a greater extent. Comparatively, BrN was included into the cavity occupied by *n*-octanol to the greatest extent and iodide ions show the least quenching effect on the phosphorescence of BrN. In the presence of TX(R), BrN exposes to bulky water phase to the greatest extent and iodide ions show the most significant quenching effect on the phosphorescence of BrN. In the case of TX, the bulky *tert*-octyl chain better fits the cavity. Close contact of BrN and the phenyl group of TX with the help of the nanocavity of  $\beta$ -CD affords better rigidity and leads to much brighter phosphorescence of BrN in aerated aqueous solutions. Effective intermolecular energy transfer between the phenyl group of TX and BrN was also observed. Particularly, strong hydrophobic interaction of BrN with flexible and low polar cyclohexyl group of TX(R) also greatly contributes to the binding of BrN to the  $\beta$ -CD:TX(R) complex, and thereby, the value of  $K_2$  for the  $\beta$ -CD:TX(R):BrN complex was larger than the stability constant of the  $\beta$ -CD:BrN complex. For this reason, the best rigidity of BrN was obtained among the supramolecular inclusion complexes. This should be the reason for the observation of brightest phosphorescence although BrN exposes to bulky water phase to the greatest extent.

#### 4. Conclusions

Fluorescence measurements of OP and TX demonstrate that the hydrophobic moiety with phenyl group of amphiphiles was included into the cavity of  $\beta$ -CD.

Amphiphiles included by  $\beta$ -CD loses their unique amphiphilicity.  $^1\text{H}$  NMR spectra provide additional evidence that the long and flexible octyl chain of amphiphiles was located inside the channeled cavity in the compressed manner. Apparent stability constants of  $\beta$ -CD complexes with amphiphiles increase in the order: *n*-octanol < OP < TX < TX(R). Comparison of molecular sizes and thermodynamic stability shows that the built-in phenyl group and the geometric fit of *tert*-octyl chain to the cavity leads to higher thermodynamic stability of  $\beta$ -CD complexes with amphiphiles. The cyclohexyl ring of TX(R) shows a greater contribution to the binding strength than the phenyl ring of OP and TX. Fluorescence and phosphorescence measurements suggest that inclusion of rigid BrN into the cavity could drive the phenyl ring of OP and TX to expose to bulk water phase to a greater extent. The inclusion depth of BrN depends on the size and binding strength of hydrophobic moiety of amphiphiles to the cavity. In the case of TX(R) with the short and bulky hydrophobic tail, strong hydrophobic interaction of BrN with flexible and low polar cyclohexyl group of TX(R) greatly increases the binding strength of BrN to the  $\beta$ -CD:TX(R) complex. The formation of compact inclusion complex greatly improves the rigidity of BrN and results in the brightest phosphorescence of the  $\beta$ -CD:TX(R):BrN complex.

### Acknowledgements

The authors would like to thank the Natural Science Foundation of Gansu Province (ZS011-A25-011-Z) and Innovation Foundation of Science and Technology of Northwest Normal University (NWNNU-KJXCXGC-02-09) for their generous financial supports.

### References

- [1] L.H. Tong, Cyclodextrin Chemistry: Fundamentals and Applications, Science Press, Beijing, 2001, pp. 330–377.
- [2] E.M. Martin Del Valle, Process. Biochem. 39 (2004) 1033–1046.
- [3] T. Okubo, H. Kitano, N. Ise, J. Phys. Chem. 80 (1976) 2661–2664.
- [4] I. Sakate, S. Yoshida, K. Hayakata, T. Maeda, Y. Kusumoto, Bull. Chem. Soc. Jpn. 59 (1986) 3991–3993.
- [5] J. Georges, S. Desmetre, J. Colloid Interface Sci. 118 (1987) 192–200.
- [6] R. Palepu, V.C. Reinsborough, Can. J. Chem. 66 (1988) 325–328.
- [7] D.J. Jobe, R.E. Verall, R. Palepu, V.C. Reinsborough, J. Phys. Chem. 92 (1988) 3582–3586.
- [8] P. Palepu, J.E. Richardson, V.C. Reinsborough, Langmuir 5 (1989) 218–221.
- [9] T. Okubo, Y. Maeda, H. Kitano, J. Phys. Chem. 93 (1989) 3721–3724.
- [10] C.D. Lavandier, M.P. Pelletier, V.C. Reinsborough, Aust. J. Chem. 44 (1991) 457–461.
- [11] N. Funasaki, H. Yodo, S. Hada, S. Neya, Bull. Chem. Soc. Jpn. 65 (1992) 1323–1330.
- [12] Y. Satio, H. Ueda, M. Abe, T. Sato, S.D. Christian, Colloids Surf. A 135 (1998) 103–108.
- [13] U.R. Dharmawardana, S.D. Christian, E.E. Tucker, R.W. Taylor, J.F. Scamehorn, Langmuir 9 (1993) 2258–2263.
- [14] J. Czapkiewicz, B. Tutaj, J. Inclusion Phenom. 16 (1993) 377–380.
- [15] M. Tuncay, S.D. Christian, J. Colloid Interface Sci. 167 (1994) 181–185.
- [16] R.H. Lu, J.C. Hao, H.Q. Wang, L.H. Tong, J. Colloid Interface Sci. 192 (1997) 37–42.
- [17] Q.X. Guo, Z.Z. Li, T. Ren, X.Q. Zhou, Y.C. Liu, J. Inclusion Phenom. 17 (1994) 149–152.
- [18] S. Hashimoto, J.K. Thomas, J. Am. Chem. Soc. 107 (1985) 4655–4662.
- [19] S.G. Nelson, I.M. Warner, Carbohydr. Res. 192 (1989) 305–312.
- [20] V.K. Smith, T.T. Ndou, A. Munoz de la Pena, I.M. Warner, J. Inclusion Phenom. 10 (1991) 471–484.
- [21] L.R. Lin, Y.B. Jiang, X.Z. Du, G.Z. Chen, Chem. Phys. Lett. 266 (1997) 358–362.
- [22] A. Data, D. Mandal, S.K. Pal, S. Das, K. Bhattacharyya, J. Chem. Soc. Faraday Trans. 94 (1998) 3471–3475.
- [23] X.Z. Du, Y.B. Jiang, X.Z. Huang, G.Z. Chen, Acta Chim. Sin. 56 (1998) 453–457.
- [24] L. Wilson, R. Verrall, Can. J. Chem. 76 (1998) 25–34.
- [25] H.J. Buschmann, E. Cleve, E. Schollmeyer, J. Inclusion Phenom. 33 (1999) 233–241.
- [26] C.H. Evans, M. Partyka, J.V. Stam, J. Inclusion Phenom. 38 (2000) 381–396.
- [27] G.M. Escandar, A. Munoz de la Pena, Appl. Spectrosc. 55 (2001) 496–503.
- [28] E.I. Popova, I.N. Topchieva, Russ. Chem. Bull. 50 (2001) 620–625.
- [29] C. Retna Raj, R. Ramaraj, Electrochim. Acta 44 (1998) 279–285.
- [30] S.G. Skoulika, C.A. Georgiou, M.G. Polissiou, J. Inclusion Phenom. 34 (1999) 85–96.
- [31] W. Eli, W.H. Chen, Q.J. Xue, J. Inclusion Phenom. 38 (2000) 37–43.
- [32] H. Gharibi, S. Jalili, T. Rajabi, Colloids Surf. A 175 (2000) 361–369.
- [33] C. Karakasyan, M. Taverna, M.C. Millot, J. Chromatogr. A 1032 (2004) 159–164.
- [34] K.A. Udachin, J.A. Ripmeester, J. Am. Chem. Soc. 120 (1998) 1080–1081.
- [35] C.H. Evans, M. Partyka, J.V. Stam, J. Inclusion Phenom. 38 (2000) 381–396.
- [36] G.X. Zhao, Physical Chemistry of Surfactants, second ed., Beijing University Press, Beijing, 1984, p. 167.
- [37] R.L. Vanetten, J.F. Sebastian, G.A. Clowes, M.L. Bender, J. Am. Chem. Soc. 89 (1967) 3242–3253.
- [38] Q.X. Guo, Z.Z. Li, T. Ren, X.Q. Zhu, Y.C. Liu, J. Inclusion Phenom. 17 (1992) 471–484.
- [39] A.J.M. Valente, M. Nilsson, O. Söderman, J. Colloid Interface Sci. 281 (2005) 218–224.
- [40] B. Tutaj, A. Ksprzyk, J. Czapkiewicz, J. Inclusion Phenom. 47 (2003) 133–136.
- [41] N. Yoshida, T. Shirai, M. Fujimoto, Carbohydr. Res. 192 (1989) 291–304.
- [42] S. Hamai, J. Am. Chem. Soc. 111 (1989) 3954–3957.